Research

Study on the synthesis and structural characterization of spinel-structured Co_3O_4 metal oxide derived from metal-organic framework materials

Nguyen Van Bang*, Nguyen Thi Phuong

Institute of Materials, Biology and Environment, Academy of Military Science and Technology, 17 Hoang Sam, Nghia Do, Hanoi, Vietnam.
*Corresponding author: vbnguyenhh@gmail.com
Received 12 May 2026; Revised 26 Jun. 2026; Accepted 10 Aug. 2026; Published 25 Aug. 2026.
DOI: https://doi.org/10.54939/1859-1043.j.mst.113.2026.81-87

ABSTRACT

Spinel Co_3O_4 materials were successfully synthesized through the thermal decomposition of Co-BTC metal-organic frameworks prepared by hydrothermal and microwave-assisted methods. The structural characteristics and physicochemical properties of the materials were investigated by XRD, EDX, FTIR, SEM, and N_2 adsorption-desorption analyses. XRD and FTIR results confirmed the complete transformation of Co-BTC into pure spinel Co_3O_4 with high crystallinity, while EDX analysis indicated the complete removal of organic components after calcination. SEM images revealed that Co-BTC exhibited rod-like crystals, whereas Co_3O_4 consisted of near-spherical nanoparticles with sizes of approximately 50-60 nm, forming a porous structure. All samples exhibited mesoporous characteristics with type IV-H3 adsorption isotherms. The Co_3O_4 sample derived from the microwave-assisted MOF precursor achieved the highest specific surface area of 80.1 m^2/g, which was significantly higher than that of the hydrothermal sample. The microwave-assisted method reduced the synthesis time to 60 min while improving the porous structure and process efficiency in accordance with green chemistry principles.

Keywords: Spinel structure; Co_3O_4; Metal-organic framework; XRD; EDX; FTIR; SEM; BET.

1. INTRODUCTION

In the context of increasing air pollution caused by the emission of volatile organic compounds (VOCs), the development of efficient, low-cost, and sustainable catalytic systems has attracted considerable attention. Among transition metal oxides, spinel-structured Co_3O_4 is considered a promising material due to its high physicochemical stability, flexible Co^{2+}/Co^{3+} redox conversion, strong oxidation activity, and lower cost compared with noble metal catalysts [1, 2]. Co_3O_4 can exist in various morphologies and microstructures, such as nanoparticles, nanorods, hollow structures, and hierarchical architectures, in which the material morphology significantly influences the specific surface area, porosity, and mass transfer properties [3, 4]. Currently, Co_3O_4 has been synthesized by various methods, including co-precipitation, sol-gel, hydrothermal synthesis, and thermal decomposition of cobalt precursors [5-7]. Although these methods can produce materials with relatively high crystallinity, simultaneous control of morphology, particle size, and pore structure remains challenging. In addition, particle agglomeration during calcination often reduces the specific surface area and porosity of the material [8, 9]. Therefore, the selection of suitable precursors to direct the structure and suppress the agglomeration of Co_3O_4 after calcination remains an important research direction.

In recent years, metal-organic frameworks (MOFs) have been regarded as promising precursors for the synthesis of metal oxides with controllable structures [10, 11]. Owing to their ordered crystalline structures, high porosity, and tunable morphology through the selection of metal ions and organic ligands, MOFs enable the formation of metal oxides that inherit the morphology of the parent framework after thermal decomposition. In particular, for Co-MOFs, thermal decomposition not only leads to the formation of spinel Co_3O_4 but also contributes to the development of porous structures and relatively uniform particle distribution [12]. Compared with

conventional synthesis methods, the MOF-derived approach offers improved control over the microstructure, reduced particle agglomeration, and larger specific surface area.

In addition, the microwave-assisted method for MOF synthesis has attracted considerable attention due to its rapid heating capability, shortened reaction time, and ability to produce crystals with small particle size and high uniformity [13, 14], which are advantageous for the conversion into porous metal oxides after calcination. In this study, spinel-structured Co_3O_4 was synthesized through the thermal decomposition of Co-BTC prepared by hydrothermal and microwave-assisted methods in order to investigate the formation of crystalline phases, structural characteristics, morphology, and pore properties of the obtained materials. The use of Co-BTC as a precursor facilitated the formation of porous Co_3O_4 with relatively uniform nanosized particles through the structural inheritance effect from the parent MOF framework.

2. EXPERIMENT AND METHOD

2.1. Chemicals, equipment and instruments

2.1.1. Chemicals

$CoCl_2 \cdot 6H_2O$ 98% (Sigma-Aldrich); 1,3,5-Benzenetricarboxylic acid 95% (H_3BTC) (Sigma-Aldrich); Ethanol ≥ 95% (Sigma-Aldrich); N, N-Dimethylformamide ≥ 99% (Sigma-Aldrich); distilled water.

2.1.2. Equipment and instruments

Glassware set (beakers, glass rods, graduated cylinders, glass funnels, etc.), magnetic stirrer with heating (HPS-20, Fcombio-USA, China), drying oven (DHG-9145A, Bluepard, China), analytical balance (PA 213, Ohaus-USA, China), Duran glass bottle (Germany), high-temperature furnace (Nabertherm GmbH, Germany), microwave oven (Electrolux, China), ultrasonic cleaner (JP-060S, Skymen, China), high-speed centrifuge (Hettich, Universal 320, Germ).

2.2. Synthesis of Co_3O_4 oxide derived from a metal-organic framework

The synthesis of Co-BTC by the microwave-assisted method was carried out by dissolving 0.015 mol of $CoCl_2 \cdot 6H_2O$ in 90 mL of a mixed solvent of distilled water/DMF/ethanol with a volume ratio of 1:1:1 under magnetic stirring until complete dissolution. Subsequently, 0.01 mol of the H_3BTC ligand was added, and the mixture was ultrasonicated for 30 min to improve dispersion and homogeneity. The resulting solution was transferred into a sealed Duran bottle and subjected to microwave treatment at 200 W for 60 min using an intermittent cycle of 5 min irradiation followed by 1 min pause. The solid product was collected by filtration, washed several times with ethanol and distilled water, and then dried at 80 °C for 5 h to obtain the Co-BTC material.

For the hydrothermal method, the initial solution preparation procedure was similar to that of the microwave-assisted method; however, the homogeneous mixture was transferred into a Teflon-lined autoclave and maintained at 150 °C for 24 h before filtration, washing, and drying at 80 °C for 5 h. Finally, the obtained Co-BTC samples were calcined in air at 400 °C for 4 h with a heating rate of 5 °C/min. After natural cooling to room temperature, Co_3O_4 cobalt oxide materials were obtained.

2.3. Material characterization methods

The morphology was examined using scanning electron microscopy (SEM), and the chemical composition was determined by energy-dispersive X-ray spectroscopy (EDX) on a Hitachi S-4800 instrument.

The phase composition of the materials was analyzed by X-ray diffraction (XRD) using an X'Pert diffractometer with CuKα radiation (λ = 1.5406 Å), operating at 45 kV and 40 mA, with a scanning rate of 0.1°/s over a 2θ range of 10° - 70°.

Functional groups and material formation were identified by Fourier-transform infrared

spectroscopy (FT-IR) using a Bruker Tensor II spectrometer.

Surface properties were determined by nitrogen adsorption-desorption isotherms (BET method) using a Novatouch LX2 instrument.

3. RESULTS AND DISCUSSION

The phase purity and crystalline characteristics of Co-BTC and the Co_3O_4 materials derived from the MOF precursors were investigated by X-ray diffraction (XRD), and the results are presented in Figure 1a. The XRD patterns of the Co-BTC samples synthesized by both hydrothermal and microwave-assisted methods exhibited sharp diffraction peaks at 2θ values of approximately 17.48°, 18.67°, 27.13°, and 35.45°, corresponding to the (220), (111), (002), and (440) crystal planes, respectively. These diffraction peaks can be indexed to the monoclinic Co-BTC framework with the space group $P2_1/c$, indicating the successful formation of highly crystalline Co-BTC.

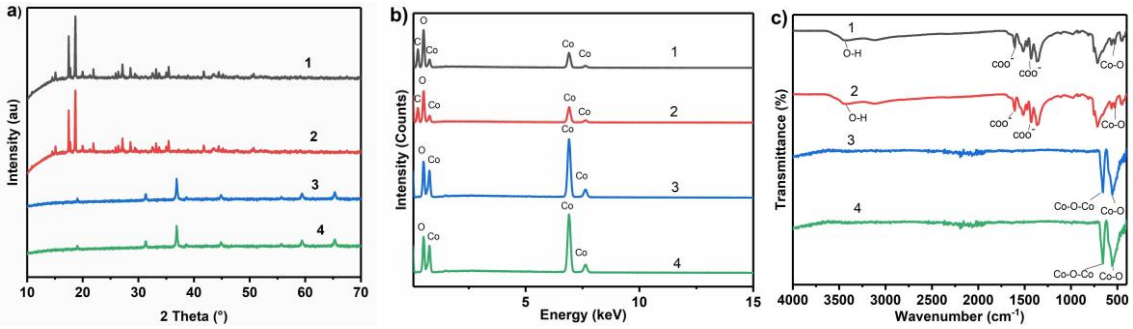

Figure 1. *XRD patterns(a), EDX spectra(b), and FTIR spectra(c) of the Co-BTC(1, 2) and Co_3O_4 (3, 4) materials: 1, 3 - Synthesized by the hydrothermal method; 2, 4 - Synthesized by the microwave-assisted method.*

After calcination, the diffraction patterns of both samples changed completely, indicating the conversion of the Co-BTC framework into cobalt oxide (Figure 1a). All diffraction peaks were well indexed to the standard pattern of spinel Co_3O_4 (PDF No. 00-042-1467), and no additional diffraction peaks attributable to impurity phases were detected within the detection limit of XRD. The characteristic reflections located at $2\theta \approx 19.0°$, 31.3°, 36.9°, 38.6°, 44.8°, 59.4°, and 65.3° correspond to the (111), (220), (311), (222), (400), (511), and (440) crystal planes, respectively, confirming the formation of the cubic spinel Co_3O_4 phase. The sharp and intense diffraction peaks further indicate the high crystallinity of the obtained oxide materials.

Table 1. *Elemental composition of the Co-BTC and Co_3O_4 oxide materials.*

Element	Hydrothermal method				Microwave-assisted method			
	Co-BTC		Co_3O_4		Co-BTC		Co_3O_4	
	Weight, %	Atomic, %	Weight, %	Atomic, %	Weight, %	Atomic, %	Weight, %	Atomic, %
C K	40.21	51.32	-	-	37.49	50.16	-	-
O K	47.25	45.27	30.53	60.73	44.49	44.69	29.23	59.30
Mn K	8.04	2.24	44.98	26.05	11.82	3.46	43.04	25.43
Co K	4.51	1.17	24.49	13.22	6.20	1.69	27.73	15.27
Totals	100							

The elemental compositions of Co-BTC and Co_3O_4 synthesized by both methods were analyzed by EDX (Table 1 and Figure 1b). The Co-BTC samples contained C, O, and Co as the major elements, consistent with the composition of the metal–organic framework. After calcination, the carbon signal was no longer detected, indicating effective decomposition of the organic ligand

during thermal treatment. Meanwhile, the cobalt content increased from approximately 19 - 23 wt.% to 73 - 74 wt.% owing to the removal of the organic component. The Co/O atomic ratio obtained from EDX was generally consistent with the expected stoichiometry of Co_3O_4. Together with the XRD results, these observations support the successful conversion of the Co-BTC precursor into spinel Co_3O_4.

The FT-IR spectra of Co-BTC synthesized by hydrothermal and microwave-assisted methods (Figure 1c) exhibited broad absorption bands at 3424 - 3108 cm^{-1}, corresponding to the stretching vibration of O–H groups from adsorbed or coordinated water molecules. The absence of the characteristic C=O stretching band of free H_3BTC (1730 - 1690 cm^{-1}) indicates deprotonation of the ligand and coordination of the carboxylate groups with Co^{2+} ions. The absorption bands at 1605 - 1515 cm^{-1} and 1429 - 1354 cm^{-1} are assigned to the asymmetric and symmetric stretching vibrations of COO^- groups, respectively, while the band at 526 cm^{-1} is attributed to Co–O vibrations, supporting the formation of the Co-BTC framework. After calcination, the characteristic organic absorption bands disappeared, and two new bands appeared at 554 and 657 cm^{-1}, corresponding to Co–O and O–Co–O lattice vibrations in spinel Co_3O_4. These spectral changes indicate the decomposition of the organic framework and the formation of cobalt oxide, in agreement with the XRD analysis.

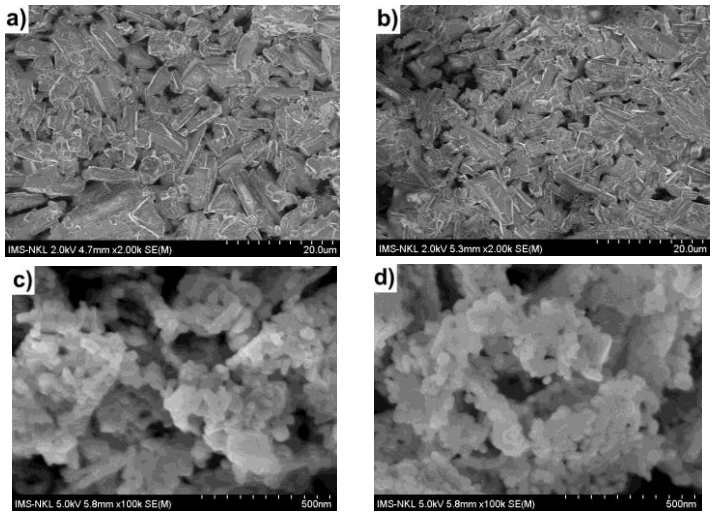

Figure 2. *SEM images of Co-BTC (a, b) and Co_3O_4 (c, d): a, c - Synthesized by the hydrothermal method; b, d - Synthesized by the microwave-assisted method.*

The SEM images (Figure 2) show that the Co-BTC samples synthesized by both hydrothermal and microwave-assisted methods consisted of relatively uniform rod-like crystals with lengths of approximately 5 - 10 μm and widths of 2 - 3 μm, indicating well-defined crystal growth during MOF synthesis. After calcination, the rod-like morphology was transformed into uniformly distributed spherical or near-spherical Co_3O_4 nanoparticles with average sizes of approximately 50 - 60 nm, forming aggregated clusters. The formation of these aggregates generated interparticle voids, which is consistent with the mesoporous characteristics revealed by the nitrogen adsorption-desorption measurements. These observations indicate that the Co-BTC precursor effectively controls the morphology of the resulting Co_3O_4 while preserving a porous particle assembly after thermal conversion.

The N_2 adsorption-desorption isotherms and pore-size distribution curves of Co-BTC and Co_3O_4 are presented in Figures 3 and 4, and the corresponding textural parameters are summarized in Table 2. Both the Co-BTC precursors and the derived Co_3O_4 materials synthesized by hydrothermal and microwave-assisted methods exhibited type IV adsorption isotherms with H3

hysteresis loops, characteristic of mesoporous materials according to the IUPAC classification. The BJH pore-size distribution further confirmed the presence of well-developed mesopores, which are mainly associated with interparticle voids formed by particle aggregation, consistent with the SEM observations.

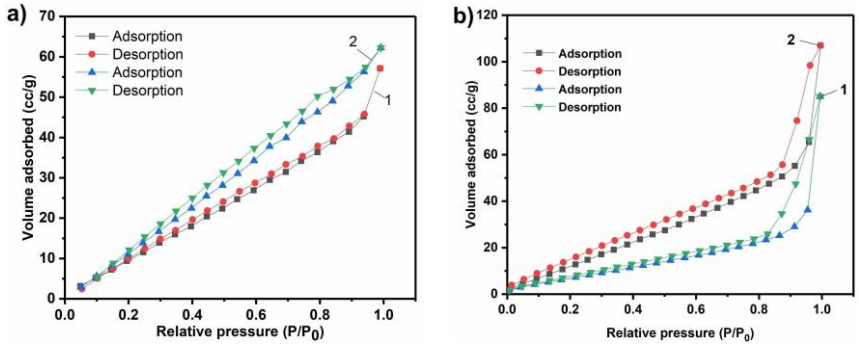

***Figure 3**. The nitrogen adsorption-desorption isotherms of Co-BTC (a) and Co_3O_4 (b): 1 - Synthesized by the hydrothermal method; 2 - Synthesized by the microwave-assisted method.*

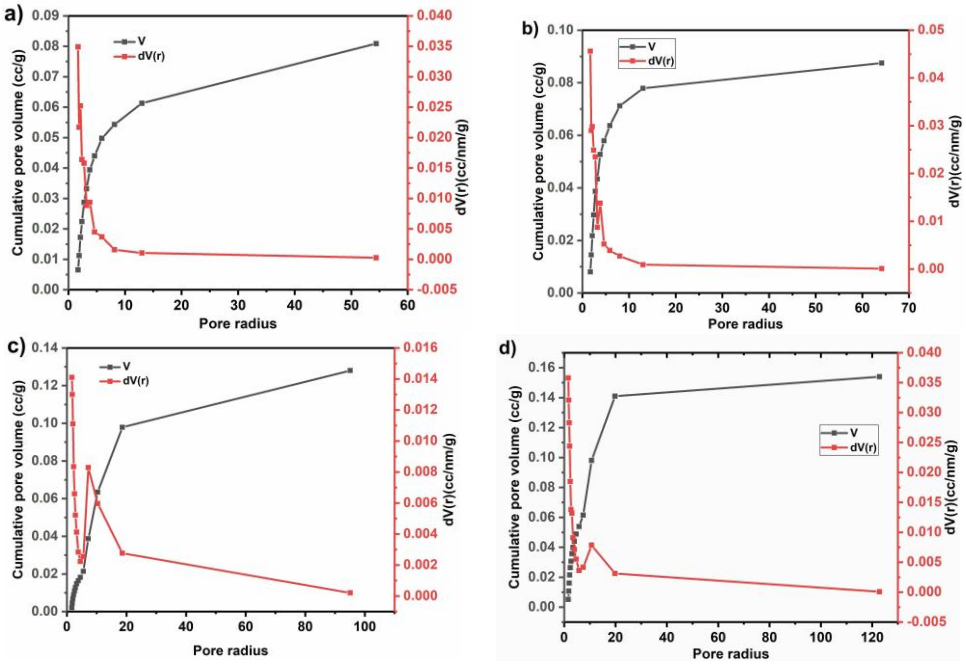

***Figure 4.** Pore size and volume distribution curve of* Co-BTC *(a, b) and* Co_3O_4 *(c, d): a, c - Synthesized by the hydrothermal method; b, d - Synthesized by the microwave-assisted method.*

As summarized in Table 2, the specific surface areas of Co_3O_4 prepared by the hydrothermal and microwave-assisted methods were 53.2 and 80.1 m^2/g, respectively, which are slightly lower than those of the corresponding Co-BTC precursors (67.7 and 99.1 m^2/g). This reduction can be attributed to framework collapse and partial pore shrinkage during thermal decomposition, together with particle aggregation during oxide formation. Nevertheless, the obtained Co_3O_4 materials retained a well-developed mesoporous structure after calcination.

Among the two synthesis routes, the microwave-assisted method produced Co_3O_4 with a considerably higher specific surface area than the hydrothermal method. The obtained surface area (80.1 m^2/g) is also higher than those reported for MOF-derived Co_3O_4 prepared by conventional hydrothermal methods (63.4 m^2/g [15] and 28.75 m^2/g [16]) and solution precipitation methods

(26.7 m^2/g [17] and 61 m^2/g [18]). This improvement may be attributed to the rapid and volumetric heating provided by microwave irradiation, which promotes more homogeneous nucleation, suppresses excessive crystal growth, and yields MOF precursors with finer particles and more developed porosity. These characteristics contribute to the higher specific surface area of the derived Co_3O_4 after calcination.

Table 2. *Main parameters obtained from nitrogen adsorption-desorption isotherm measurements of Co-BTC and MOF-derived Co_3O_4.*

Parameter	Hydrothermal method		Microwave-assisted method	
	Co-BTC	Co_3O_4	Co-BTC	Co_3O_4
Specific surface area (BET), m^2/g	67.7	53.2	99.1	80.1
Pore diameter, nm	3.38	3.34	3.38	3.24
Pore volume, cm^3/g	0.081	0.128	0.088	0.154

Overall, Co_3O_4 was successfully synthesized from Co-BTC precursors prepared by microwave-assisted synthesis within only approximately 60 min, representing a substantial reduction compared with the conventional hydrothermal route. The shorter synthesis time is expected to improve process efficiency while reducing energy consumption and operational costs. Moreover, the reduced processing time contributes to a more sustainable synthesis process that is consistent with the principles of green chemistry.

4. CONCLUSIONS

Co_3O_4 materials were successfully synthesized by calcination of Co-BTC precursors prepared via hydrothermal and microwave-assisted methods. XRD, EDX, and FTIR analyses consistently demonstrated the successful conversion of the Co-BTC precursors into spinel Co_3O_4. SEM observations revealed that the rod-like Co-BTC crystals (5 - 10 μm) were transformed into near-spherical Co_3O_4 nanoparticles with average sizes of approximately 50 - 60 nm after calcination, accompanied by the formation of interparticle pores resulting from nanoparticle aggregation. All Co_3O_4 samples exhibited mesoporous characteristics with type IV isotherms and H3 hysteresis loops. The Co_3O_4 sample derived from the microwave-assisted Co-BTC precursor exhibited the highest specific surface area (80.1 m^2/g), which was significantly higher than that of the hydrothermally derived sample (53.2 m^2/g). Furthermore, the microwave-assisted method reduced the preparation time of the Co-BTC precursor to approximately 60 min, providing a rapid and energy-efficient route for the synthesis of porous Co_3O_4 materials.

Acknowledgement: *This study was conducted with financial support from the 2025 Ministry of Industry and Trade-level science and technology project. Contract No.039.2025.ĐT.BO/HĐKHCN.*

REFERENCES

[1]. Fan Dang et al., *"Advances in metal oxide catalysts for efficient VOCs oxidation: Synthesis strategy and catalytic mechanism"*, Chinese Journal of Catalysis, 8, pp. 97-123, (2026).

[2]. Xiao Song et al., *"Facet-dependent catalytic mechanism of Co_3O_4 for VOCs oxidation: Role of tetra-coordinated co on (220) Planes"*, Volume 707, 139779, (2026).

[3]. Jinze Lyu et al., *"Comparative study on Co^{3+}, Co^{2+}, and oxygen vacancies in the photocatalytic ozonation of VOCs on Co_3O_4 crystal facets"*, Volume 363, Part 1, 132072, (2025).

[4]. Amaya Gil-Barbarin et al., *"Viability of strontium carbonate-modified Co_3O_4 catalysts for chlorinated VOCs oxidation"*, Journal of Environmental Chemical Engineering, Volume 12, Issue 6, 114402, (2024).

[5]. J. Lei et al., *"Mesoporous Co_3O_4 derived from facile calcination of octahedral Co-MOFs for toluene catalytic oxidation"*, Industrial & Engineering Chemistry Research, 59, pp. 5583–5590, (2020).

[6]. Q. Ren et al., *"1D-Co_3O_4, 2D-Co_3O_4, 3D-Co_3O_4 for catalytic oxidation of toluene"*, Catalysis Today, 332, pp. 160 - 167, (2019).

[7]. M. Zhang et al., *"Macroscopic hexagonal Co_3O_4 tubes derived from controllable two-dimensional metal-organic layer single crystals: formation mechanism and catalytic activity"*, Inorganic Chemistry, 59, pp. 3062 - 3071, (2020).

[8]. Do Thi Thuy et al., *"Tổng hợp nanocomposite khung cơ kim Ce/graphen oxit biến tính octyl amin (Ce-Imi/GO-OA) ứng dụng chế tạo lớp phủ bảo vệ chống ăn mòn kim loại"*, Journal of Military science and technology, no. FEE, pp. 231-236, (2024) (in Vietnamese).

[9]. X. Zhu et al., *"Co_3O_4 nanoparticles with different morphologies for catalytic removal of ethyl acetate"*, Catalysis Communications, 156, pp. 106320, (2021).

[10]. Nguyen Quang Huy et al., *"Synthesis of MIL-101(Cr) metal-organic framework material and research photocatalytic capability of material for nitrate removal in water"*, Journal of Military Science and Technology, 101, pp. 102-109, (2025).

[11]. Yibo Wang et al., *"Ligand-tailored Co-O bond strength in MOF-derived Co_3O_4 for boosting NO oxidation"*, Separation and Purification Technology, Volume 377, Part 3, 134482, (2025).

[12]. Jiaqi Li et al., *"Efficient dexamethasone photocatalytic mineralization via heterojunction construction of Co_3O_4 derived from MOF and ultrathin carbon nitride"*, Separation and Purification Technology, Volume 386, 136539, (2026).

[13]. Li, S. et al., *"Three-dimensional porous carbon/Co_3O_4 composites derived from graphene/Co-MOF for high-performance supercapacitor electrodes"*, Applied Surface Science, 503, 144090, (2020).

[14]. Zhao, J. et al., *"Controlled porous hollow Co_3O_4 polyhedral nanocages derived from metal-organic frameworks (MOFs) for toluene catalytic oxidation"*, Molecular Catalysis, 463, pp. 77-86, (2019).

[15]. Juan Lei et al., *"Mesoporous Co_3O_4 Derived from Facile Calcination of Octahedral Co-MOFs for Toluene Catalytic Oxidation"*, Ind. Eng. Chem. Res., 59, pp. 5583-5590, (2020).

[16]. Jinwu Hua et al., *"MOF-derived porous Co_3O_4 nanosheets array assembled on SnO_2 nanofibers for humidity-resistant high efficiency acetone detection"*, Chinese Chemical Letters, 37, 110863, (2026).

[17]. Guanghui Zhang et al., *"Pore-size modulation of MOF-derived hollow porous Co_3O_4 toward high-performance for xylene gas sensors"*, Vacuum, 233, 114047, (2025).

[18]. Amensisa Negasa Begia et al., *"Low-concentration H_2S gas sensors based on MOF-derived Co_3O_4 nanomaterials"*, Sensors & Actuators: A. Physical, 378, 115776, (2024).

TÓM TẮT

Nghiên cứu tổng hợp và đánh giá đặc trưng cấu trúc của vật liệu oxit kim loại cấu trúc spinel Co_3O_4 trên cơ sở vật liệu khung kim loại-hữu cơ

Vật liệu Co_3O_4 spinel được tổng hợp thành công thông qua nhiệt phân khung cơ-kim Co-BTC điều chế bằng phương pháp thủy nhiệt và hỗ trợ vi sóng. Đặc trưng cấu trúc và tính chất vật liệu được khảo sát bằng XRD, EDX, FTIR, SEM và hấp phụ-giải hấp phụ N_2. Kết quả XRD và FTIR xác nhận sự chuyển hóa hoàn toàn của Co-BTC sang pha Co_3O_4 tinh khiết có cấu trúc spinel và độ kết tinh cao, phân tích EDX cho thấy thành phần hữu cơ đã bị loại bỏ hoàn toàn sau nung. Ảnh SEM cho thấy Co-BTC có dạng tinh thể hình que, trong khi Co_3O_4 gồm các hạt nano gần cầu kích thước khoảng 50-60 nm tạo cấu trúc xốp. Các mẫu đều có hệ mao quản trung bình với đường đẳng nhiệt kiểu IV-H3. Co_3O_4 tổng hợp từ MOF bằng hỗ trợ vi sóng đạt diện tích bề mặt riêng cao nhất 80,1 m^2/g, lớn hơn đáng kể so với mẫu thủy nhiệt. Phương pháp hỗ trợ vi sóng giúp rút ngắn thời gian tổng hợp xuống 60 phút, đồng thời cải thiện cấu trúc xốp và hiệu quả quy trình theo hướng hóa học xanh.

Từ khoá: Cấu trúc spinel; Co_3O_4; Vật liệu khug kim loại-hữu cơ; XRD; EDX; FTIR; SEM; BET.